

Valence-band maximum in the layered semiconductor WSe₂: Application of constant-energy contour mapping by photoemission

Th. Straub, K. Fauth, Th. Finteis, M. Hengsberger, R. Claessen,* P. Steiner, and S. Hüfner
Fachrichtung Experimentalphysik, Universität des Saarlandes, D-66041 Saarbrücken, Germany

P. Blaha

Institut für Technische Elektrochemie, Technische Universität Wien, A-1060 Wien, Austria

(Received 12 January 1996; revised manuscript received 6 March 1996)

Angular-resolved photoemission data and a full-potential fully relativistic density-functional calculation on the electronic band structure of the layered semiconductor WSe₂ consistently show that the valence-band maximum is located at the sixfold-degenerate *K* point of the Brillouin zone and not at its center, as earlier calculations have predicted. By mapping out constant energy contours with photoemission spectroscopy, the *k* space location of the valence-band maximum can be visualized in a very instructive way, demonstrating the potential of this spectroscopic technique also for semiconductors. [S0163-1829(96)50724-1]

WSe₂ is a semiconducting material with a layered crystal structure consisting of hexagonal Se-W-Se sandwiches separated by van der Waals gaps. With its fundamental band gap of about 1.2 eV matching well the solar spectrum and due to its remarkable stability against photocorrosion, WSe₂ has been proposed as a promising material for photovoltaic applications.¹ Indeed, electrochemical devices based on WSe₂ have been reported to possess conversion efficiencies of up to 17%.² Furthermore, recent studies using scanning tunneling microscopy revealed that by applying short-time voltage pulses to the tunneling tip stable, readable, and erasable surface modifications on a nanometer or even atomic scale can be created on WSe₂ surfaces.³

Despite these interesting macroscopic properties only little work on the underlying microscopic electronic structure is reported in the literature. From optical experiments the nature of the fundamental band gap has been identified as indirect.⁴ Photoelectron spectroscopy has been applied to study the metal-semiconductor interface formation and properties on WSe₂,⁵ but, to our knowledge, no angle-resolved photoemission data on the $\epsilon(\mathbf{k})$ band structure of the bare surface exist so far. Apart from a few tight-binding calculations, only one density-functional-type band structure calculated within the local-density approximation (LDA) has been published.⁶ This calculation, which uses the augmented spherical wave (ASW) method, confirms the indirect nature of the gap with the valence-band maximum (VBM) localized at the center of the Brillouin zone (BZ), i.e., at the Γ point (see Fig. 2 for the BZ of WSe₂), and the lowest unoccupied state half-way along the ΓK line.

In this paper we present data from angle-resolved photoelectron spectroscopy (ARPES) and the results of a full-potential LDA band calculation, which consistently place the highest occupied valence-band state at the *K* point of the BZ, in striking contrast to the earlier prediction. We demonstrate the usefulness of a new spectroscopic technique, namely, the mapping of constant-energy contours by photoemission, for the determination and visualization of the VBM in (layered) semiconductors. A comprehensive discussion of our ARPES and LDA results of the electronic structure of WSe₂ will be presented elsewhere.⁷

For our band calculation we have used the full-potential linear augmented-plane-wave (LAPW) method,⁸ including local orbitals for the high-lying “semicore” states. Exchange and correlation are treated within the LDA; self-consistency was reached using scalar-relativistic equations. In the final iteration spin-orbit coupling was included as perturbation. In contrast to the ASW calculation of Coehoorn *et al.*,⁶ no shape approximation to potential or charge density was made, and this may explain the small but important differences between their and the present work. Our calculation was performed for the experimentally determined crystal structure, even though a total-energy optimization yielded a slightly smaller (by 4%) W- to Se-layer separation.

The resulting band structure is shown in Fig. 1. Here we want to focus on the topmost valence-band states. Near the zone center (Γ/A) the highest occupied states consist of mostly W $5d_{z^2}$ orbitals with some Se $5p_z$ character mixed in. Since these orbitals are oriented perpendicular to the layer structure, the corresponding bands display a noticeable energy dispersion along the ΓA line of the BZ. When following these bands towards the zone edge, it changes its orbital

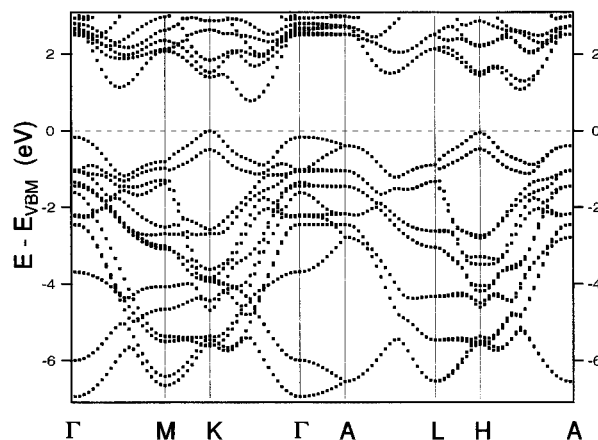


FIG. 1. LDA band structure for various high-symmetry directions (energies relative to the valence-band maximum).

character completely. For example, near the K point the highest valence-band states are derived from in-plane orbitals ($W 5d_{xy}$ and $5d_{x^2-y^2}$ in equal weights). As a consequence, their energy dispersion along KH is almost negligible.

The most interesting result of our calculation is that the topmost valence-band state at the K point is found 170 meV higher in energy than the highest occupied state at the zone center (Γ). This is in striking contrast to the calculation of Ref. 6, which places the VBM at Γ , by almost 500 meV above the topmost state at K . We should add here that our finding of the VBM at K is independent of the inclusion of spin-orbit coupling. The conduction-band minimum (CBM) is found about half-way along ΓK , here being in good agreement with Ref. 6. Our new calculation thus confirms the indirect character of the fundamental band gap. However, transitions across the gap have to occur between the K point and the CBM at $\approx 1/2\Gamma K$, and not between Γ and the CBM as thought before.

The photoemission measurements have been performed with He-I (21.22 eV) radiation (at the home laboratory in Saarbrücken) and with synchrotron light (at BESSY, Berlin). In both cases a VG ESCALAB spectrometer was used. The home system was equipped with a fully automated manipulator, which allows an independent variation of the azimuthal and polar angles of photoelectron detection. Thus a large fraction of the 2π half-space above the sample can be scanned.⁹ Two spectroscopic methods have been employed, namely, the measurement of energy distribution curves (EDC's) and the mapping of constant-energy contours (CEC's) (described below). For both techniques an analyzer acceptance angle of $\pm 1.75^\circ$ ($\pm 1.0^\circ$ at BESSY) and an energy resolution of 100 meV was used. Intrinsically p -doped WSe_2 crystals were grown using the chemical vapor transport method. For the photoemission measurements fresh surfaces were prepared by *in situ* cleavage. Characterization of surface quality and orientation of the crystals was achieved by using photoelectron diffraction patterns and the azimuthal symmetry of the EDC's.

In Fig. 2(a) we show a selection of He-I excited EDC's measured along the ΓK (AH) azimuth. Focusing on the topmost features we find around normal emission ($\theta \approx 0^\circ$) an asymmetric peak, which towards higher emission angles develops into a characteristic double peak around 17.5° . Concerning its energy position the topmost structure disperses upwards from normal emission, assumes its maximum energy around 38° [corresponding to the K (H) point in the BZ], and moves down again for higher emission angles. The spectra additionally contain an extrinsic energy shift to larger binding energies, presumably caused by a Fermi-level shift due to adsorbate-induced defect states in the gap, which was carefully monitored by repeatedly measuring normal emission EDC's throughout the ΓK (AH) series.¹² Taking the resulting band bending into account, the energy separation between the topmost peak in the 0° spectrum and that at K (H) is found to be 850 ± 50 meV, which was consistently reproduced on several samples. This is best seen in the inset of Fig. 2(a) which contains spectra at 0° and 38° , both measured immediately after cleavage, so that the Fermi-level shift can be safely neglected in this case. Peak energies in the EDC's measured along other high-symmetry directions⁷ also

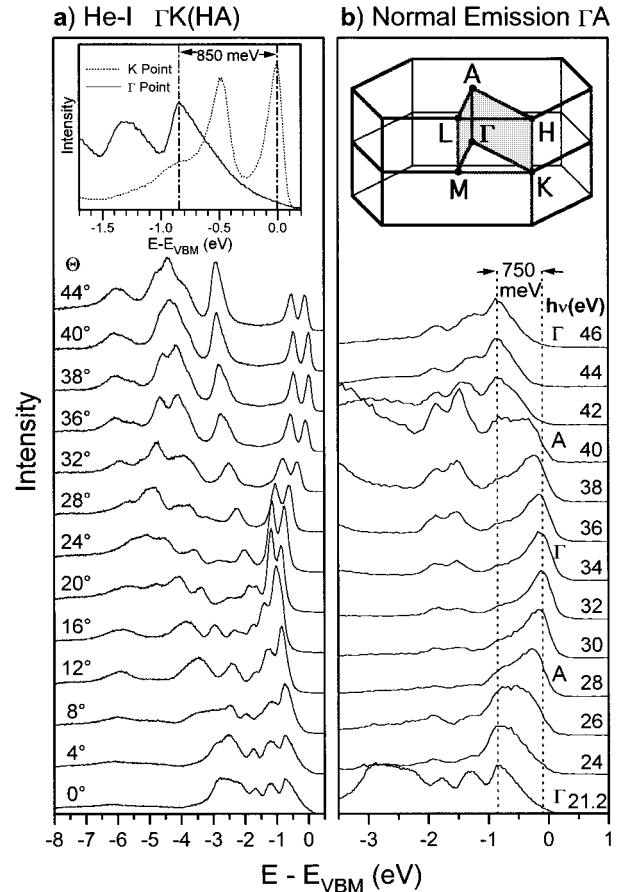


FIG. 2. (a) Selected He-I excited EDC's along ΓK (AH). Binding energies relative to the VBM. Spectra are corrected for He-I satellite emission, but not for band bending (see text). The inset shows spectra at Γ ($\theta=0^\circ$) and K (38°) both measured immediately after crystal cleavage. (b) Normal emission spectra excited with synchrotron radiation showing the dispersion along the ΓA direction of the BZ. Spectra are corrected for band bending. Also shown is the Brillouin zone of WSe_2 with critical points.

remain clearly below that of the topmost emission at K (H). Thus, the valence-band peak with the highest energy along the ΓK (AH) azimuth is observed at the K (H) point. For this reason we have deliberately chosen its position as energy zero, because, as we will discuss below, this state can be identified with the VBM.

Figure 3 contains a comparison of the high-lying experimental bands derived from the EDC's in Fig. 2(a) with a projection of our theoretical bulk band structure onto the surface BZ.¹⁰ Especially around the K (H) point the qualitative behavior of the experimental dispersions is nicely reproduced by the LDA bands. The observed energy separation of the double peak of the order of 500 meV has to be compared to the splitting predicted by the LDA calculation of 300–490 meV along ΓK and AH . Towards Γ (A) the two topmost LDA bands display a rapidly increasing k_\perp dependence, with only one intense spectral structure (namely, the asymmetric peak mentioned above) falling into the now broadened projected density of states along ΓA . The fact that, experimentally, the second band is not clearly resolved can be understood from the following discussion.

As seen in Fig. 1 the LDA calculation predicts the two

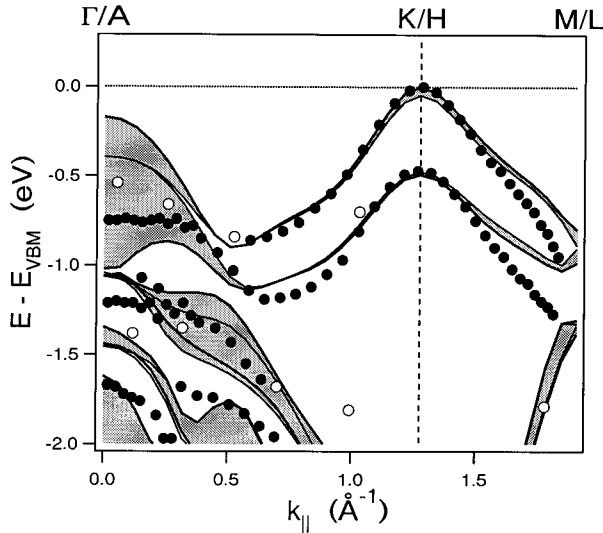


FIG. 3. Experimental band structure (dots) measured along the ΓK (AH) azimuth compared with the corresponding LDA bulk band structure projected onto the ΓK ($k_{\perp}=0$) line of the surface BZ (shaded area). Open dots denote weak spectral structures. The experimental points are raw data not yet corrected for the band bending.

highest valence bands to be degenerate at A and split by 850 meV at Γ . From normal emission spectra measured with synchrotron radiation [displayed in Fig. 2(b)] and using an inner potential of 14.5 eV as determined by comparison with the band calculation and independently by target current spectroscopy⁷ we conclude that the \mathbf{k} -space location of the 0° He-I spectra is close to a Γ point in the extended zone scheme. It can be shown that photoemission selection rules related to the nonsymmorphic space group (D_{6h}^4) of WSe_2 (Ref. 11) allow excitations from the second band, but suppress emission from the highest state at this wave vector, leaving it only as a tail-like emission centered at about 100 meV binding energy in the He-I spectrum. The synchrotron spectra further show that, when tuning the photon energy into the next BZ ($h\nu \approx 34$ eV), the intensity is now shifted to the highest state at Γ , while emission from the second one becomes suppressed, in accordance with the selection rules.¹¹ From these data we determine a full separation of the first and second valence-band state at Γ of 750 meV, in good agreement with the location of the weak shoulder relative to the main peak in the He-I spectrum.

This discussion demonstrates that, even though the energies of the intense peaks in the He-I EDC's in Fig. 2 already seem to suggest that the VBM is located at the K point, a more careful interpretation taking into account the effects of transition matrix elements is required. We nevertheless arrive at the same conclusion, with the topmost state at K about 100 ± 50 meV higher in energy (i.e., lower in binding energy) than that at the Γ point, thus confirming the result of our LDA calculation.

A very instructive way of visualizing the position of the VBM in reciprocal space can be achieved by performing the photoemission experiment in a different mode. Rather than keeping the electron emission angle fixed and scanning its kinetic energy as in the EDC's, we now keep the energy constant (i.e., we accept photoelectrons only within a fixed

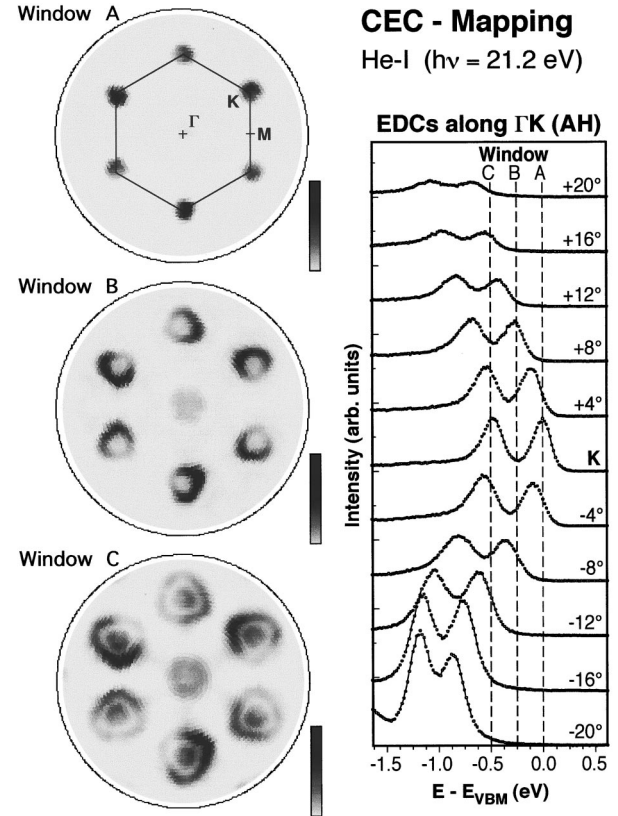


FIG. 4. CEC maps for binding energies of 0 (A), 250 (B), and 500 meV (C) relative to the VBM. The panel on the right shows the corresponding energy positions in the EDC's measured around the K (H) point of the BZ.

energy window given by the analyzer resolution) and measure the intensity as a function of the emission direction over almost the entire half-space above the sample surface. Translating the emission angle into the in-plane wave vector \mathbf{k}_{\parallel} and neglecting possible \mathbf{k} -space modulations of transition probabilities, one thus maps out the occupancy of states at a given energy in reciprocal space, or, in other words, one measures constant energy contours (CEC) $\varepsilon(\mathbf{k}_{\parallel}) = \text{const}$. This technique has previously been used to measure Fermi surfaces in metals.^{13,14} To our knowledge, this is the first time it is utilized for the determination of the VBM in a semiconductor.

In Fig. 4 we show CEC maps for three different energies near the top of the valence band. Map A has been obtained for the highest photoelectron energy for which photoemission intensity can be detected, i.e., it corresponds to zero binding energy relative to the VBM. It displays intense spots centered around the six equivalent K (H) points of the BZ, thus nicely visualizing the \mathbf{k} -space position of the VBM. As the binding energy is increased by 250 meV (map B), the spots develop into hollow rings, whose intensity distribution reflects the threefold symmetry of the surface layer¹⁵ more clearly than map A . The ring shape is easily understood from the EDC's also shown in Fig. 4: at 250 meV below the VBM the topmost band has moved away from K (H) in all directions, whereas at the K (H) point itself the detection energy now falls exactly into the gap between the first and second peak. Additionally, new intensity appears at the BZ center (Γ/A), originating from the weak shoulder visible in the 0°

spectrum of Fig. 2(a). Map *C* finally shows the CEC for a binding energy of 500 meV. Now the topmost band has moved further out, giving rise to the triangularly shaped rings, while the maximum of the second-highest band appears at *K* (*H*) at this energy. Also, the intensity at Γ (*A*) increases strongly, because the intense first peak observed in the 0° EDC is beginning to enter the energy window of the analyzer.

In conclusion, both our photoemission and LDA results place the VBM of WSe_2 at the sixfold degenerate *K* point of the BZ. This is of importance for the understanding of the transport properties of *p*-doped WSe_2 , because the additional possibility of intervalley scattering will affect carrier lifetimes and mobilities. Furthermore, the essential in-plane

($5d_{xy}$ and $5d_{x^2-y^2}$) character of the valence states at *K*, as obtained in the band calculation, accounts well for the observed transport anisotropy.¹⁶ The application of constant energy contour mapping allows us to visualize the position of the VBM in reciprocal space in a very instructive way, thus demonstrating the potential of this new photoemission technique also for semiconductors.

We wish to thank the group of E. Bucher (Konstanz) for the WSe_2 single crystals and J. Osterwalder (Zürich) and P. Aebi (Fribourg) for sharing with us the technology for CEC mapping. We are also indebted to M. Lux-Steiner (Berlin) for helpful discussions on WSe_2 . This work was supported by the DFG (SFB 277 and Hu 149/17-1).

* Author to whom correspondence should be addressed.

¹H. Tributsch, *Z. Naturforsch. Teil A* **32**, 972 (1977).

²G. Prasad and O. N. Srivastava, *J. Phys. D* **21**, 1028 (1988).

³H. Fuchs, R. Laschinski, and Th. Schimmel, *Europhys. Lett.* **13**, 307 (1990).

⁴K.-K. Kam, C.-L. Chang, and D. W. Lynch, *J. Phys. C* **17**, 4031 (1984).

⁵A. Klein, C. Pettenkofer, W. Jaegermann, M. Lux-Steiner, and E. Bucher, *Surf. Sci.* **321**, 19 (1994), and references therein.

⁶R. Coehoorn, C. Haas, J. Dijkstra, C. J. F. Flipse, R. A. de Groot, and A. Wold, *Phys. Rev. B* **35**, 6195 (1987).

⁷K. Fauth *et al.* (unpublished).

⁸P. Blaha, K. Schwarz, P. Dufek, and R. Augustyn, computer code WIEN-95, TU WIEN 1995 [improved and updated UNIX version of the original copyrighted WIEN code, published by P. Blaha, K. Schwarz, P. Sorantin, and S. B. Trickey, *Comp. Commun.* **59**, 399 (1990)].

⁹An identical setup is described in D. Naumovic, A. Stuck, T. Greber, J. Osterwalder, and L. Schlapbach, *Phys. Rev. B* **47**, 7462 (1993).

¹⁰Knowledge about the momentum component perpendicular to the surface is very limited, because it is a *nonconserved* quantity in photoemission. Therefore we compare experimental band dis-

persions to the *projected* theoretical bulk band structure. The k_\perp uncertainty is much less of a problem when perpendicular band dispersions can be neglected, as, e.g., for the highest valence bands along the *KH* line in WSe_2 (cf. Figs. 1 and 3).

¹¹D. Pescia, A. R. Law, M. T. Johnson, and H. P. Hughes, *Solid State Commun.* **56**, 809 (1985).

¹²Similar shifts occurred also in the synchrotron measurements, but here it was possible to correct them by aligning the spectra to the non- k_\perp -dispersive peak at -1.8 eV [cf. Fig. 2(b)].

¹³A. Santoni, L. J. Terminello, F. J. Himpsel, and T. Takahashi, *Appl. Phys. A* **52**, 299 (1991).

¹⁴P. Aebi, J. Osterwalder, R. Fasel, D. Naumovic, and L. Schlapbach, *Surf. Sci.* **307-309**, 917 (1994).

¹⁵Though the overall bulk symmetry of the space group D_{6h}^4 is sixfold, a single Se-W-Se sandwich, being accessible with the low escape depth of the He-I-excited photoelectrons, has only threefold symmetry. The observation of this reduced symmetry also reflects the high surface perfection of the cleaved WSe_2 crystals, as will be discussed in Ref. 7 and in Th. Straub *et al.* (unpublished).

¹⁶M. K. Agarwal, P. D. Patel, and O. Vijayan, *Phys. Status Solidi A* **78**, 103 (1983).